CHAPTER IV

STRUCTURAL ASPECTS OF MESOPOROUS AlPO$_4$-5 (AFI) ZEOTYPE USING MICROWAVE RADIATION AND ALUMATRANE PRECURSOR

4.1 Abstract

A new route for preparation of mesoporous AlPO$_4$-5 (AFI) zeotype has been synthesized using alumatrane precursor, prepared from aluminum hydroxide and triisopropanolamine (TIS) by the Oxide One Pot Synthesis (OOPS), via microwave technique using triethylamine (TEA) as a structure-directing agent. The influences of the reaction mixture composition, HF acid, water content and the crystallization temperature and time were investigated. The prepared materials were characterized using X-ray diffraction, SEM and BET. The results showed a mesoporous AlPO$_4$-5 zeotype having a uniform rod-like structure with surface area around 120–180 m^2/g. The high crystallinity with narrow size distribution of crystals was obtained at a high amount of structure-directing agent (the mole ratio of TEA/Al$_2$O$_3$ = 3.5). The presence of fluorine ion retarded the nucleation and growth rate, leading to a bigger crystal size. The crystal of the AFI grew preferentially in the c-direction with the reaction time and the water content. The use of lower reaction temperature to obtain good crystalline material can be compensated by a longer reaction time.

4.2 Introduction

Aluminophosphate molecular sieves, known as AlPO$_4$-n (n refers to a distinct structure type) and built from alternating (AlO$_4$)$^-$ and (PO$_4$)$^+$ tetrahedra linked together to form a neutral framework [1], are useful in a number of applications; in particular as catalysts and catalyst supports. In addition, the aluminophosphates have been shown to possess interesting ion exchange and adsorption properties. Among them, a well known AlPO$_4$-5 molecular sieve with an AFI type framework has one-dimensional 12-membered-ring channels parallel to the c-axis with a pore diameter in micropore region of 0.73 nm [1], and shows excellent thermal stability. AFI has

attracted much attention due to its zeolitic properties, use in catalysis, and potential applications, such as host matrix to organize dye molecules for nonlinear optics [2]. Incorporation of a small amount of Si [3] or metal, such as VAPO-5 [4], [Ni]APO-5 [5], [Cr]APO-5 [6] into AFI framework can change their acidity and catalytic activities. The aluminophosphates are generally prepared under conventional hydrothermal heating conditions [7–9] with a reaction time ranging from several hours to several days. It is known that the AFI type can be synthesized by using several types of structure-directing agents; for example TEA [7], TEAOH [10], TPA [8], TPAOH [11] and TBAOH [9]. However, a new synthesis technique combining hydrothermal and microwave heating was also employed for the preparation of microporous $AlPO_4$-5 zeotype [10, 12–16] due to a reduction of the crystallization time [6]. Moreover, microwave heating apparently uniforms crystal size distribution [17], provides a higher phase purity [15] and phase selective crystallization by getting rid of unstable materials [4, 18]. These results are from higher heating rate, faster dissolution of the gel and a more homogeneous heating by microwave irradiation compared with conventional heating. Although the microporous $AlPO_4$-5 has been developed by several groups, its micropore still causes diffusion limitation. Recently, a new family of crystalline zeolitic materials, so-called mesoporous zeolite single crystals, was reported to overcome this problem [19–21]. These materials combine the benefits of mesoporous molecular sieves and zeolites. The mesopore improves the mass transfer to and form the active sites. These mesoporous zeolites are found to enhance catalytic properties as compared to conventional zeolites [22, 23]. The synthesis of mesoporous AFI has been reported using cation exchange resin beads [21] or by introducing carbon into reaction mixtures via fluoride route [20].

In Wongkasemjit's group [24–26], alumatrane containing a trialkanoamine ligand has been used successfully as a source of aluminum for the synthesis of zeolite via the sol-gel process and microwave technique. Thus, in this work, alumatrane, directly synthesized from aluminium hydroxide and TIS (triisopropanolamine) via the Oxide One Pot Synthesis (OOPS), was chosen as a precursor for synthesizing mesoporous aluminophosphate with $AlPO_4$-5 (AFI)-type structure via microwave heating technique.

4.3 Experimental

4.3.1 Materials Characterization

Powder X-ray diffraction (XRD) patterns were carried out using a Rigaku X-ray diffractometer with CuKα as a source in a range from 5 ° to 50 ° was a step of 5 °/min. Functional groups of materials were followed using an FTIR spectrophotometer (Nicolet, NEXUS 670) with a resolution of 4 cm^{-1}. Thermogravimetric analysis (TGA) was carried out using TG-DTA (Pyris Diamond Perkin Elmer) with a heating rate of 10°C/min in the range of room temperature to 750 °C under nitrogen atmosphere to determine the thermal stability. The BET surface area measurement, pore volume, and pore size distribution were measured using nitrogen at 77 K in an Autosorb-1 gas sorption system (Quantasorb JR). Morphology was studied on a JEOL 5200-2AE scanning electron microscope. Calcination was conducted using a Carbolite furnace (CFS 1200) with a heating rate of 1 °C/min at 600 °C. Hydrothermal crystallization by microwave heating technique was carried out using Milestone's Ethos Microwave Solvent Extraction Lab-station. The frequency of the microwave radiation was 2.45 GHz. The crystallinity of the samples was determined from the XRD pattern diffraction data using the following equation

$$\% \text{ crystallinty } = (\Sigma I / \Sigma I_s) * 100$$

where I is the line intensity of the sample and I_s is the line intensity of the standard sample. The standard sample is the sample with the highest crystallinity and no amorphous as identified by XRD and supported by SEM. The line intensities of the XRD pattern at 2θ = 7.5, 14.9, 19.8, 21.1, 22.5 and 26.0 [7] were employed for these calculations.

4.3.2 Methodology

4.3.2.1 Synthesis of Alumatrane

The preparation of alumatrane or tris(alumatranyloxy-*i*-propyl)amine, followed the work of Wongkasemjit *et al.* [27] via the Oxide One Pot Synthesis (OOPS) process. Aluminium hydroxide (Sigma Chemical Co., 0.1 mole), TIS (Aldrich Chemical Co. Inc., USA, 0.125 mole) and ethylene glycol (EG from J.T. Baker, Inc., Phillipsburg, USA, 100 mL) were added to a 250 mL two-necked round bottom flask. The mixture was homogeneously stirred at room temperature before being heated to 200 °C under nitrogen in an oil bath for 10 h. Excess EG was removed under vacuum (10^{-2} Torr) at 110°C to obtain the crude product. The crude solid was washed with acetonitrile (Lab-Scan Company Co., Ltd.) and dried under vacuum at room temperature. Dried products were characterized using TGA and FTIR.

FTIR: 3700–3300 cm^{-1} (v OH), 2750–3000 cm^{-1} (v CH), 1650 cm^{-1} (v OH overtone), 1460 cm^{-1} (δ CH), 1078 cm^{-1} (v Al–O–C) and 500–800 cm^{-1} (v Al–O). TGA: 33 % ceramic yield which is larger than the theoretical value, 23.7 %. This may be due to the incomplete combustion, as confirmed by the black color of the char.

4.3.2.2 Synthesis of AlPO$_4$-5 (AFI)-type

The AlPO$_4$-5 was prepared using triethylamine [(C$_2$H$_5$)$_3$N:TEA from Fisher Scientific] as a structure-directing agent. Alumatrane was mixed with 1M phosphoric acid solution (Merck) and homogeneously stirred at room temperature, followed by adding TEA and various specified amounts of water. HF (Merck) was added successively to the gel. The mixture was stirred until becoming homogeneous before transferring to a Teflon-lined vessel sealed with a Teflon cap contained in a microwave for further heating at a reaction temperature range of 180 °–200 °C for 0.5–2 h. The product was washed and dried, followed by calcining at 600 °C for 7 h. Amount of structure-directing agent, amount of water, microwave time, and temperature were varied.

4.4 Results and Discussion

In this work, $AlPO_4$-5 with AFI structure containing 12-membered rings was prepared using the alumatrane precursor as a source of alumina and TEA as the structure-directing agent via microwave technique. It was found that the structure and morphology depend on the gel compositions, and the microwave temperature and time. As reported in reference 12, the precursor equilibrium in the gel is temperature dependence. To stabilize the reaction gel, it was necessary to mix the gel at low temperature (0 °C) to obtain a better quality of $AlPO_4$-5. However, in our case, the gel was obtained at room temperature, probably due to our home-made alumatrane being moisture stable. All the $AlPO_4$-5 samples synthesized from the alumatrane precursor had only rod-like morphology in a wide range of condition reactions. Wan *et al.* [7] explained that the $AlPO_4$-5 crystals with hexagonal rod-like or platelets which is typical for AFI type materials were formed due to more template trapped within their channels; otherwise, spherical morphology samples were formed, using low mole fraction of template. The results from the SEM images of $AlPO_4$-5 obtained, and discussed later, show perfect surface of typical rod-like crystals with no holes or pits found, as also observed by Weib *et al.* [28] when prepared $AlPO_4$-5 crystals using $Al(OH)_3$ as a source of aluminum via a conventional heating with crystallization period of 20 h at 180 °C and Rakoczy *et al.* [29] who synthesized $AlPO_4$-5 by reflux aluminum triisopropanolate as the alumina source before conventional heating at 180 °C for 5 days. Both groups, moreover, needed to add ethanal into the synthesis mixture to reduce hold or pits [28, 29]. The X-ray powder diffraction pattern of the synthesized $AlPO_4$-5 after calcination (Figure 4.1) indicates the AFI structure without any impurity, as compared to those published in the literature [14, 15].

4.4.1 Effect of template content

A mixture composition of $Al_2O_3:P_2O_5:xTEA:750H_2O$ heated at 200 °C microwave temperature for 1 h was used to investigate the effect of template concentration on the crystallization of $AlPO_4$-5. The amount of TEA, x, was varied from 1–3.5, and the results from the SEM images (Figure 4.2) show that at high TEA

concentration the crystal-size becomes smaller, with even distribution. The reason is that the higher TEA concentration, the more nuclei that are responsible for the faster nucleation; and subsequent crystallization are formed, coincident with the work done by Du $et\ al.$ [10] who reported that an increase in the gel pH due to an increase in the concentration of structure-directing agent accelerated the nucleation rate and leaded to the formation of small crystals with a narrow crystal-size distribution. However, it is known that $AlPO_4$-34 denoted as CHA and AFI compete each other during the synthesis using TEA structure-directing agent; and the content of CHA increases with an increase of pH or the TEA content [30]. Jiang $et\ al.$ [31] also reported that if too much structure-directing agent was added, not all molecules are dissolved in the solution, leading to a rough morphology of the crystals. To increase the crystal homogeneity, a suitable amount of the structure-directing agent at the mole ratio of $TEA/Al_2O_3 = 3.5$ was thus selected to control the morphology of the AFI crystals without any impurity phase for further study of other effects.

4.4.2 Effect of water content

Du et al. [10] stated that the dilution of the reaction gel decreased the nucleation rate. The effect of the water content on the formation of $AlPO_4$-5 crystals was thus investigated in this present study by fixing the mixture composition at $Al_2O_3:P_2O_5:3.5TEA:xH_2O$ at 200 °C microwave temperature for 1 h and varying the water content, x, at 500, 750, and 1000, as shown in the results in Figure 4.3 a-c, respectively. It was found that the water content indeed affected the nucleation and growth rate. The lowest water content showed a non-uniform crystal structure due to the non-homogeneity of the condensed gel. On increasing the water content to 750, more uniform crystals were obtained. However, a further increase to 1000 generates elongated and tiny rod-like crystals with some broken crystals. This phenomenon can be explained that increasing the water content in the synthesis mixture suppresses the nucleation rate and favors one-dimensional growth along the c-axis of the AFI framework, as reported by the Karanikolos and Iwasaki groups [32, 33]. These results are also confirmed by the growth curves of the AFI synthesized at different water contents in the synthesis mixture (Figure 4.4). The aspect ratio (length-per-

width) of the samples is increased as increasing the ratio of H_2O/Al_2O_3. The same results were obtained even when HF was added (Figure 4.3 d-e). However, the HF addition provided cleaner and bigger crystals (Figure 4.3d), when compared with Figure 4.3b, the mixture without HF. HF improves the solubility of the starting gel by readily coordinating fluoride to aluminum ions, resulting in aluminum expansion of the coordination sphere from four to six [34]. Moreover, the fluoride ions also prefer to behave as bidentate ligands linking two aluminum ions in the structure [34]; that is, fluoride ions impart a structure-directing template by interacting with the framework [35]. After the reaction, fluoride ions can be easily and completely removed upon calcination, and aluminum becomes 4-coordination. According to Jiang *et al.* [31] describe that the fluoride ions formed bonds with both Al and P. After hydrolysis, both Al and P were eventually release during crystallization. The slow rates of nucleation and crystallization lead to larger sized crystals having fewer defects.

It is worth noting that in this study $AlPO_4$-5 could be synthesized in a more dilute reaction mixture without any impurity phase. Unlike the study conducted by others [15], it showed that when the $H_2O:Al_2O_3$ mole ratio in the reaction mixture was increased beyond 300, the tridymite phase in the XRD results occurred.

The results of the FTIR spectra in Figure 4.5 show the same patterns for $AlPO_4$-5 synthesized without (a) and with (b) HF acid. The data exhibit typical characteristics of $AlPO_4$-5 at 470 and 630 cm^{-1} assigned to double ring and the O–P–O bending vibration [7]. The peaks at about 710 and 1120 cm^{-1} are attributed to the P–O stretching vibration of $(PO_4)^{3-}$ and the stretching vibration of Al–O in combination with P–O [36], respectively. The absence in the spectra of symmetric and asymmetric stretching of Al-F bond at 755 and 887 cm^{-1} [37] indicated that all fluorines were removed after the calcinations.

4.4.3 Effect of reaction time

The composition of $Al_2O_3:P_2O_5:3.5TEA:750H_2O$ was used to investigate the effect of reaction time on the crystallization of $AlPO_4$-5 without the addition of HF. The reaction duration was varied from 1, 1.5, and 2 h at 190 °C microwave

temperature (see Figure 4.6). For the relationship between the crystal size and the reaction time, it was found that prolonging heating duration resulted in longer crystals at all microwave temperatures (180 ° and 200 °C (results are not shown). These results are in good agreement with those cited in references [17, 33]. Kodaira *et al.* [17] found the growth in *c*-direction during the synthesis time due to the decrease of the synthesis mixture concentration. These results are also observed in our case, as clearly seen in the XRD patterns (Figure 4.7), showing the crystallinity of the samples synthesized at 190 °C for 1, 1.5, and 2 h. It showed the longer reaction time results in the higher intensity of XRD pattern, indicating the higher crystalline. The spectra show the XRD pattern of AFI growing preferentially in the *c*-direction with the reaction time. It can be seen that for the higher ratio of *c*-axis to *a* or *b*-axis, the relative diffraction intensities of the h k l planes of {0 0 2} to {1 0 0} decrease in accordance with previous result studied by Jhung *et al.* [3] who reported that the relative XRD intensity of {0 0 2}/{1 0 0} plane decreased as the crystal grew in the *c*-axis.

4.4.4 Effect of reaction temperature

Various crystallization temperatures were studied on the systems without HF by fixing the composition at $Al_2O_3:P_2O_5:3.5TEA:750H_2O$ for 1 h reaction time. The SEM images in Figure 4.8 show that the higher the reaction temperature is, the better the crystal shape with lower amorphous is. At 180 °C temperature, there was not enough energy for crystals to form. An amorphous material mixed with AFI crystals was obtained. These results are confirmed by the XRD patterns shown in Figure 4.9. At 180 °C the XRD pattern (Figure 4.9a) shows the characteristics of $AlPO_4$-5 along with a broad amorphous background. The peak intensities increase as temperature increases, implying that an increase of temperature leads to better crystallinity, as calculated their % crystallinity values in Table 4.1.

The addition of HF acid was also investigated at various temperatures and times (Figure 4.10). It was found that the higher the microwave temperature used the shorter the microwave time needed to achieve perfect crystals. At 200 °C, the crystals of $AlPO_4$-5 were obtained in only 1 h reaction time, and became longer and

bigger. At lower temperatures, 190 ° and 180 °C, heating duration for the synthesis was prolonged to 1.5 and 2 h, respectively. Jiang *et al.* [31] reported that the crystal size increased with increasing the reaction temperature. In our case, the crystal size was also increased with the reaction time, as discussed above. It can be concluded that the use of a lower microwave temperature could be compensated by a longer reaction time to obtain good crystalline $AlPO_4$-5.

4.4.5 Nitrogen physisorption

Figure 4.11 illustrates the nitrogen adsorption isotherm and the pore size distribution of the $AlPO_4$-5 sample prepared from the mixture composition of Al_2O_3:P_2O_5:3.5TEA:750H_2O at 200 °C reaction temperature for 1 h without HF. The pore size distribution and isotherm have type IV isotherm containing a hysteresis loop at relative pressures (P/P$_0$) higher than 0.4, representing mesoporous materials [20]. The product has a BET surface area around 120–180 m^2/g with average pore size distribution of about 150 Å. The physisorption for all samples also gave similar results, corresponding to mesoporous materials (not shown). This higher surface area may be resulted from TIS molecules generated from the hydrolysis of the alumatrane in the synthesis mixture. The TIS molecules could be used as a co-template in the synthesis to stabilize structure formation, the same as other alkanoamines; for example, triethanolamine [$N(CH_2CH_2OH)_3$] which can be used as a stabilizing and buffering or complexing agent in the synthesis of zeolite crystals [38] and $AlPO_4$-5 [39]. TIS possesses hydroxyl groups on the second carbon atom, thus preserving somewhat the geometry of the triethanolamine molecule, while altering the length of the alkyl chains. In addition, alcohol groups act as a reagent in the sol-gel process [25] and effectively couple with the microwave field contributing to the heating [12]. It may be concluded that triethylamine structure-directing agent and TIS from the alumatrane constrained in the unidimensional 12-ring pore channels generated larger pores, giving mesoporous $AlPO_4$-5.

4.5 Conclusions

An alumatrane precursor synthesized by the OOPS process has been successfully used to synthesize mesoporous $AlPO_4$-5 with a perfect rod-like AFI structure via microwave technique. The results show that the morphology can be controlled by varying the composition of the reaction mixture, the addition of HF acid, the crystallization time and temperature. The crystal of AFI grows preferentially in the c-direction with reaction time and in the diluted reaction mixture. The use of a lower reaction temperature to obtain a good crystalline material can be compensated by a longer reaction time.

4.6 Acknowledgements

4.7 References

1. S.T. Wilson, B.M. Lok, C.A. Messina, T.R. Cannan, E.M. Flanigen, J. Am. Chem. Soc. 104 (1982) 1146.

2. J. Caro, G. Finger, J. Kornatowski. J. Richter-Mendau. L. Werner,B. Zibrowius, Adv. Mater. 4 (1992) 27.

3. S.H. Jhung, J.S. Chang, D.S. Kim, S.E. Park, Micropor. Mesopor. Mater. 71 (2004) 135.

4. S.H. Jhung, J.H. Lee, J.W. Yoon, J.S. Hwang, S.E. Park, J.S. Chang, Micropor. Mesopor. Mater. 80 (2005) 147.

5. J.M. Jehng and C.M. Chen, Catal. Lett. 77 (2001) 147.

6. S.C. Laha, G. Kamalakar, R. Glaser, Micropor. Mesopor. Mater. 90 (2006) 45.

7. Y. Wan, C.D. Williams, C.V.A. Duke, J.J. Cox, Mater. Chem. 10 (2000) 2857.

8. Z. Guo, C. Gua, Q. Jin, B.D. Ding, J. porous mater. 12 (2005) 29.

9. F.Y. Jiang, Z.K. Tang, J.P. Zhai, J.T. Ye, J.R. Han, Micropor. Mesopor. Mater. 92 (2006) 129.

10. H. Du, M. Fang, W. Xu, X. Meng, W. Pang, J. Mater. Chem. 7 (1997) 551.

11. J.P. Zhai, Z.K. Tang, Z.M. Li, I.L. Li, F.Y. Jiang, P. Sheng, X. Hu, Chem. Mater. 18 (2006) 1505.

12. I. Girnus, K. Jancke, R. Vetter, J. Richter-Mendau, J. Caro, Zeolites. 15 (1995) 33.

13. I. Girnus, M.M. Pohl, J.R. Mendau, M. Schneider, M. Noack, D. Venzke, J. Caro, Adv. Mater. 7(8) (1995) 711.

14. M. Fang, H. Du, W. Xu, X. Meng, W. Pang, Micro. Mater. 9 (1997) 59.

15. S. Mintova, S. Mo, T. Bein, Chem. Mater. 10 (1998) 4030.

16. S.H. Jhung, J.S. Chang, Y.K. Hwang, J. Mater. Chem. 14 (2004) 280.

17. T. Kodaira, K. Miyazawa, T. Ikeda, Y. Kiyozumi, Micropor. Mesopor. Mater. 29 (1999) 329.

18. J.W. Yoon, S.H. Jhung, Y.H. Kim, S.E. Park, J.S. Chang, Bull.Korean chem. Soc. 26(4) (2005) 558.

19. C.J.H. Jacobsen, C. Madsen, J. Houzvicka, I. Schmidt, A. Carlsson, J. Am. Chem. Soc. 122 (2000) 7116.

20. K. Egeblad, M. Kustova, S.K. Klitgaard, K. Zhu, C.H. Christensen, Micropor. Mesopor. Mater. 101 (2007) 214.

21. V. Naydenov, L. Tosheva, O.N. Antzutkin, J. Sterte, Micropor. Mesopor. Mater. 78 (2005) 181.

22. C.H. Christensen, K. Johannsen, I. Schmidt, C. H. Christensen, J. Am. Chem. Soc. 125 (2003) 13370.

23. F.S. Xiao, L. Wang, C. Yin, K. Lin, Y. Di, J. Li, R. Xu, D.S. Su, R. Schlogl, T. Yokoi, T. Tatsumi, Angew. Chem. Int. Ed. 45 (2006) 3090.

24. P. Phiriyawirut, R. Magaraphan, A.M. Jamieson, S. Wongkasemjit, Micropor. Mesopor. Mater. 64 (2003) 83.

25. M. Sathupunya, E. Gulari, S. Wongkasemjit, J. Eur. Ceram. Soc. 23 (2003) 1293.

26. M. Sathupunya, E. Gulari, S. Wongkasemjit, Mater. Chem. Phys. 83 (2004) 89.

27. Y. Opornsawad, B. Ksapabutr, S. Wongkasemjit, R.M. Laine, J. Eur. Polym. 37 (2001) 1877.

28. O. Weib, G. Ihlein, F. Schuth, Micropor. Mesopor. Mater. 35-36 (2000) 317.

29. R.A. Rakoczy, S. Ernst, M. Hartmann, Y. Traa, J. Weitkamp, Catal. Today 49 (1999) 261.

30. Y. Xu, J. Maddox, J.W. Couves, J. Chem. Soc. Faraday Trans. 86 (1990) 425.

31. F.Y. Jiang, J.P. Zhai, J.T. Ye, J.R. Han, Z.K. Tang, J. Crystal Growth 283 (2005) 108.

32. G.N. Karanikolos, J.W. Wydra, J.A. Stoeger, H. Garcia, A. Corma, M. Tsapatsis, Chem. meter. 19(4) (2007) 792.

33. A. Iwasaki, T. Sano, T. Kodaira, Y. Kiyozumi, Micropor. Mesopor. Mater. 64 (2003) 145.

34. R. Szotak, Molecular Sieves, Vol. 1 (1998) 157.

35. N. Rajic, J. Serb. Chem. Soc. 70(3) (2005) 371.

36. C.M. Chen, J.M. Jehng, Catal. Lett. 85 (2003) 73.

37. M. J. Almond, Annu. Rep. Prog. Chem., Sect. C: Phys. Chem. 93 (1996) 3.

38. E.N. Coker, J.C. Jansen, Molecular Sieves, Vol 1. (1998) 121.

39. S.T. Wilson, B.M. Lok, E.M. Flanigen, US Pat. 4 310 440 (1982).
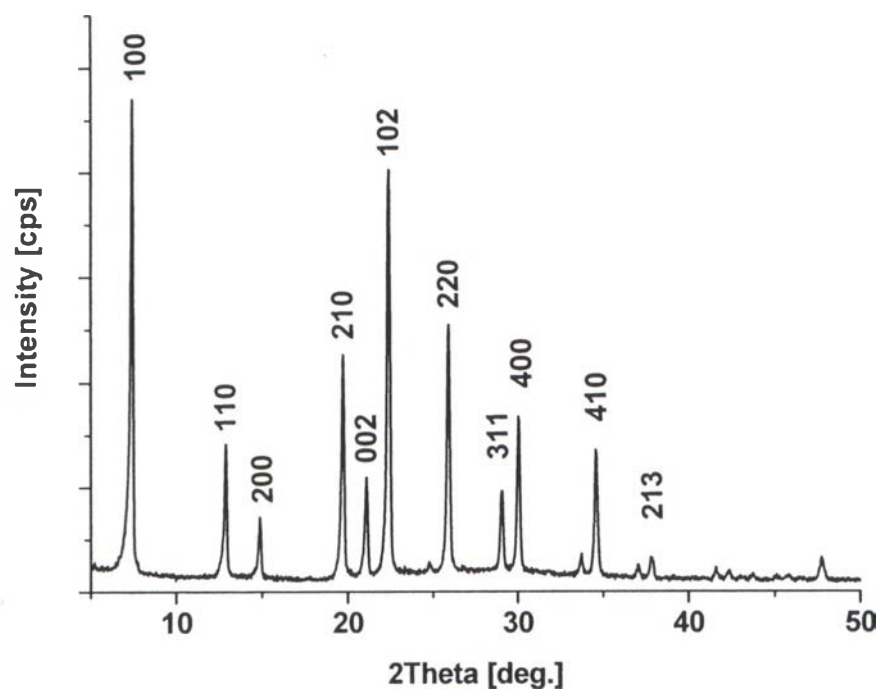
Figure 4.1   XRD pattern of the sample prepared from the mixture of $Al_2O_3:P_2O_5$: 3.5TEA:750H_2O at 200 °C for 1 h.
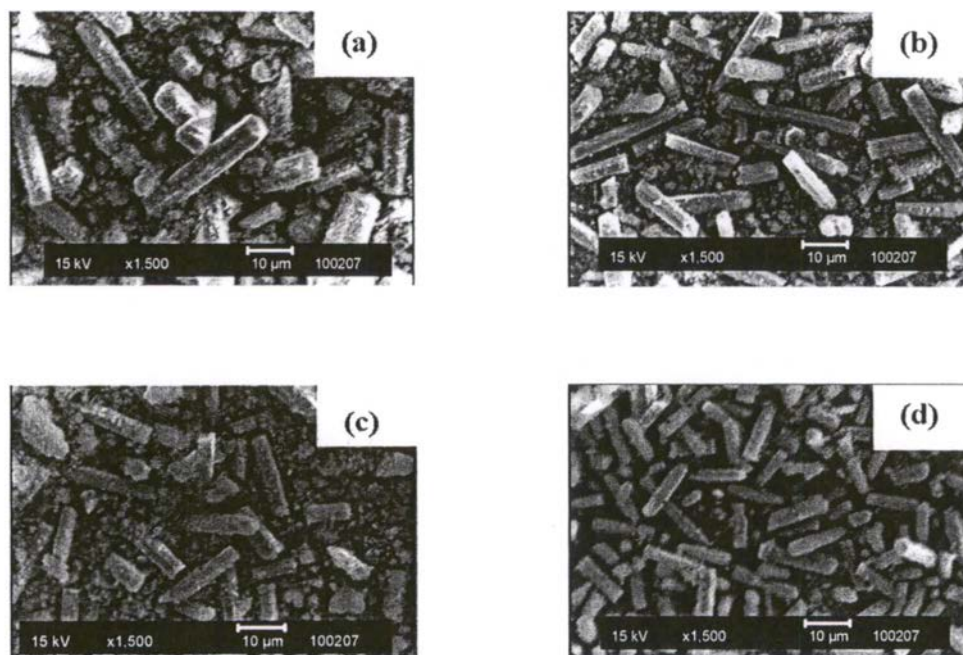
Figure 4.2   SEM images of AFI prepared from the mixture of Al_2O_3:P_2O_5:xTEA: 750 H_2O at 200 °C for 1 h where x is a) 1, b) 1.5, c) 2.5, and d) 3.5.
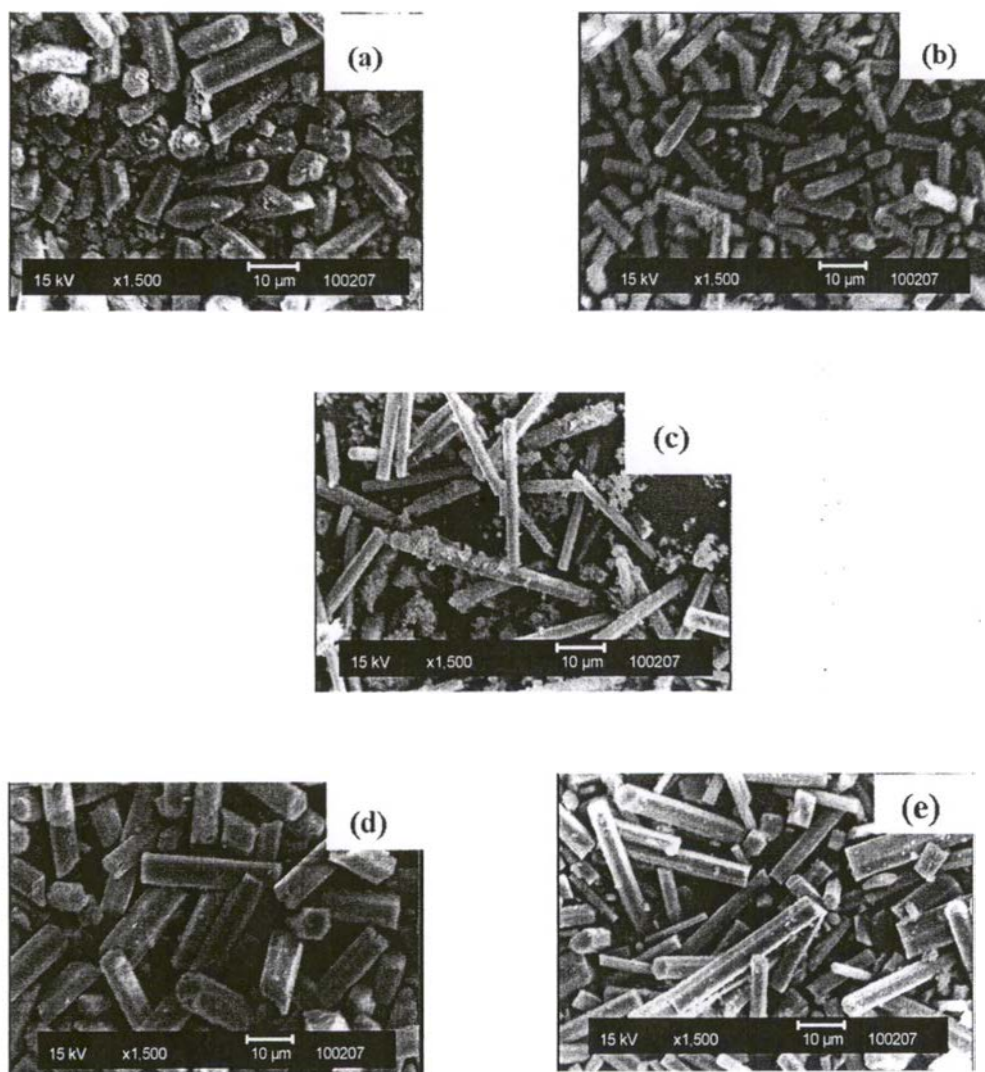
Figure 4.3 SEM images of AFI prepared from the mixture of Al_2O_3:P_2O_5: 3.5TEA:xH_2O at 200 °C for 1 h where x is a) 500, b) 750, c) 1000, d) 750 with HF acid, and e) 1000 with HF acid.
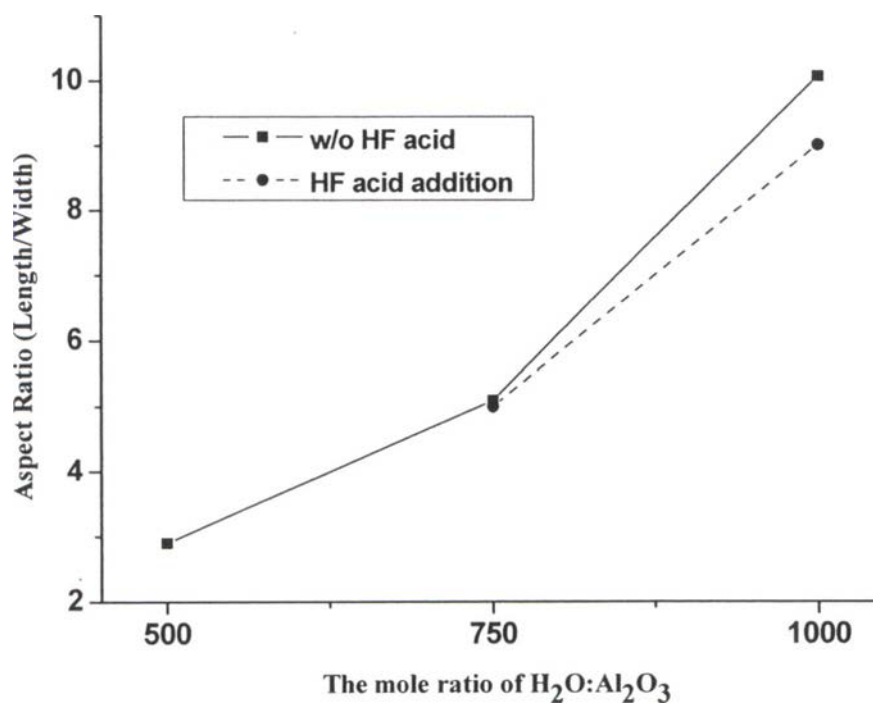
Figure 4.4   Growth curve of the AFI prepared at different the mole ratios of H_2O to Al_2O_3.
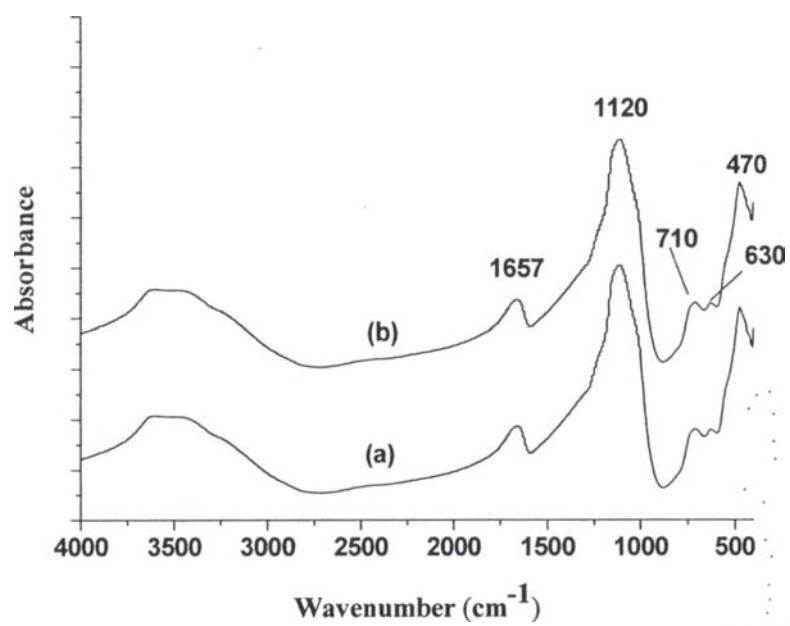
Figure 4.5 FTIR spectra of the AlPO₄-5 samples prepared from the mixture of Al_2O_3: P_2O_5: 3.5TEA:750H_2O at 200 °C for 1 h; a) without, and b) with HF acid.
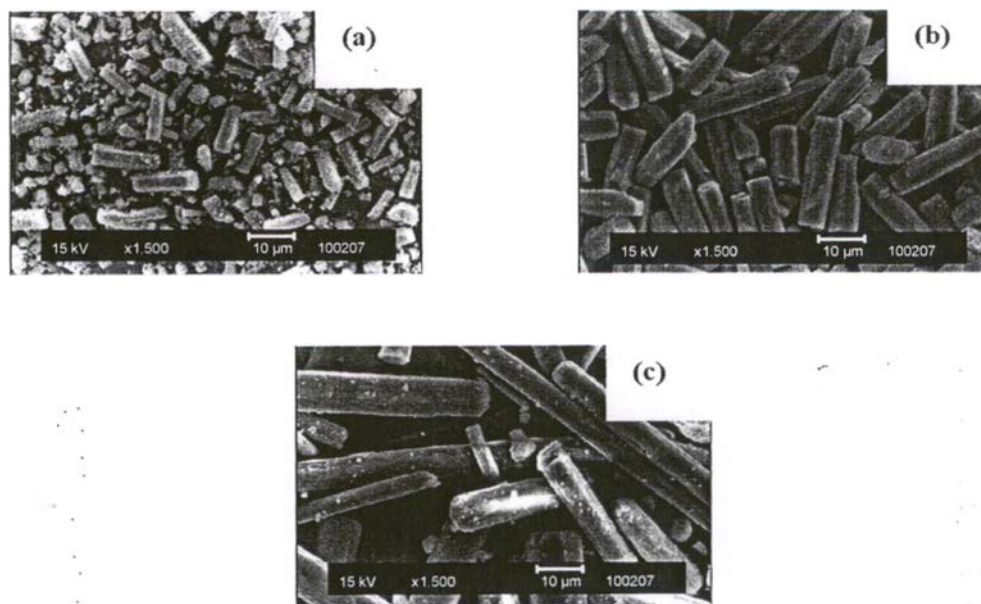
Figure 4.6   SEM images of AFI prepared from the mixture of Al_2O_3:P_2O_5: 3.5TEA:750H_2O at 190 °C microwave temperature for a) 1, b) 1.5, and c) 2 h.
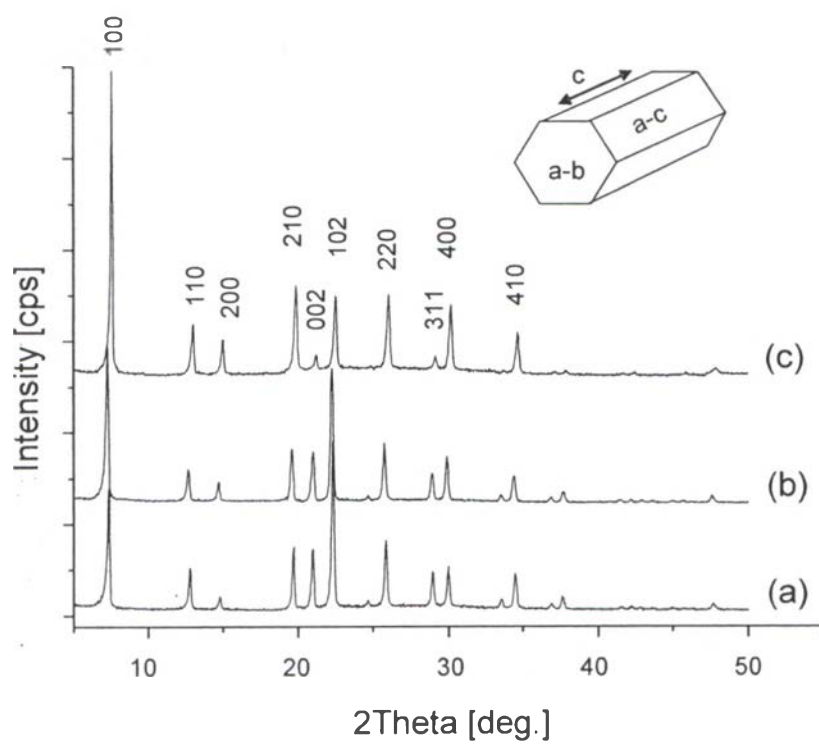
Figure 4.7 XRD patterns of the samples prepared from reaction mixtures of the composition Al_2O_3:P_2O_5:3.5TEA:750H_2O with HF acid at reaction temperatures of 190 °C for a) 1, b) 1.5, and c) 2h.
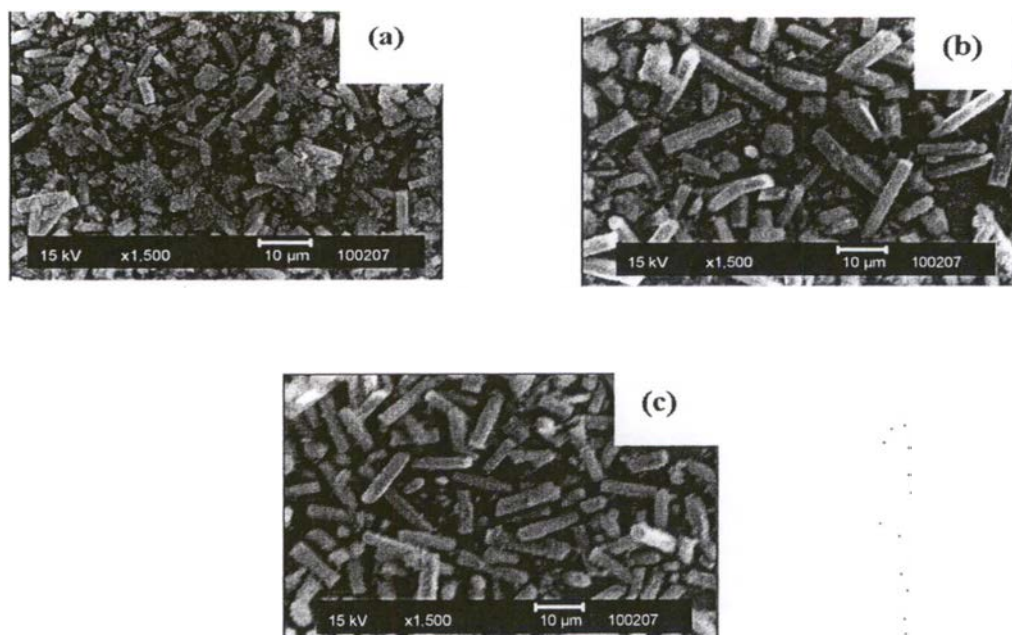
Figure 4.8   SEM images of AFI synthesized from the mixture of Al_2O_3:P_2O_5:3.5TEA:750H_2O for 1 h at microwave temperature of a) 180 °, b) 190 °, and c) 200 °C.
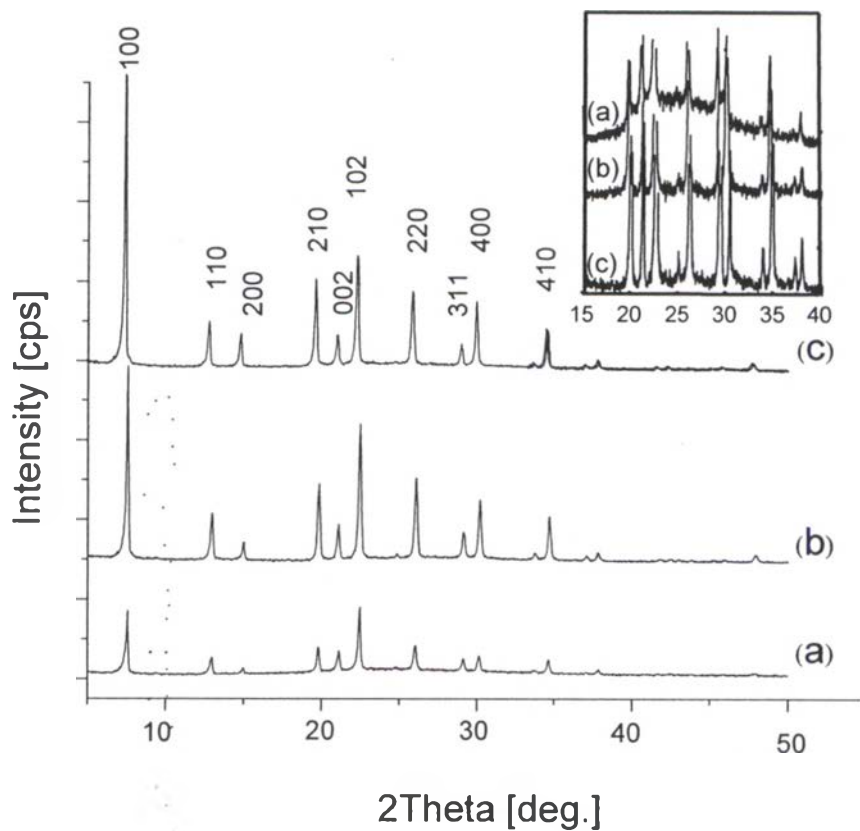
Figure 4.9 XRD patterns of AFI synthesized from the mixture of Al_2O_3:P_2O_5: 3.5TEA:750H$_2$O for 1 h at microwave temperature of a) 180 °, b) 190 °, and c) 200 °C.
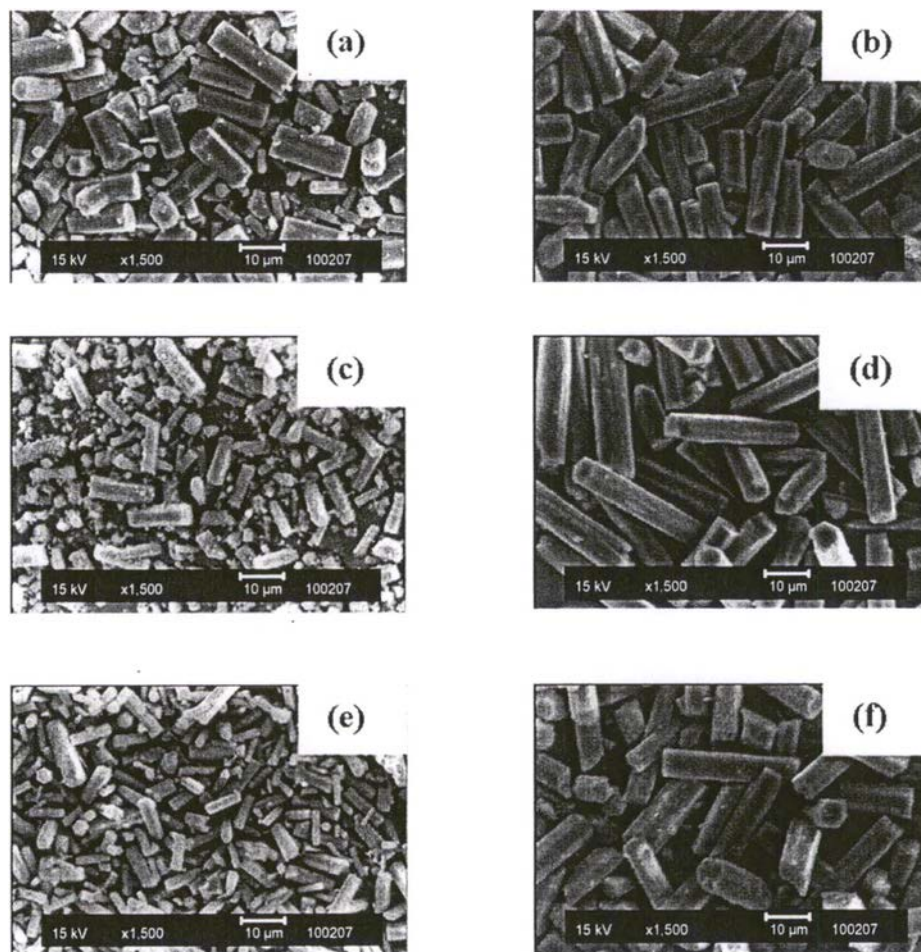
Figure 4.10 SEM images of samples prepared from the mixture of Al_2O_3:P_2O_5:
3.5TEA:750H_2O with addition of HF at microwave temperature (°C)/
time (h) of a) 180 °/1, b) 180 °/2, c) 190 °/1, d) 190°/1.5, e) 200 °/0.5,
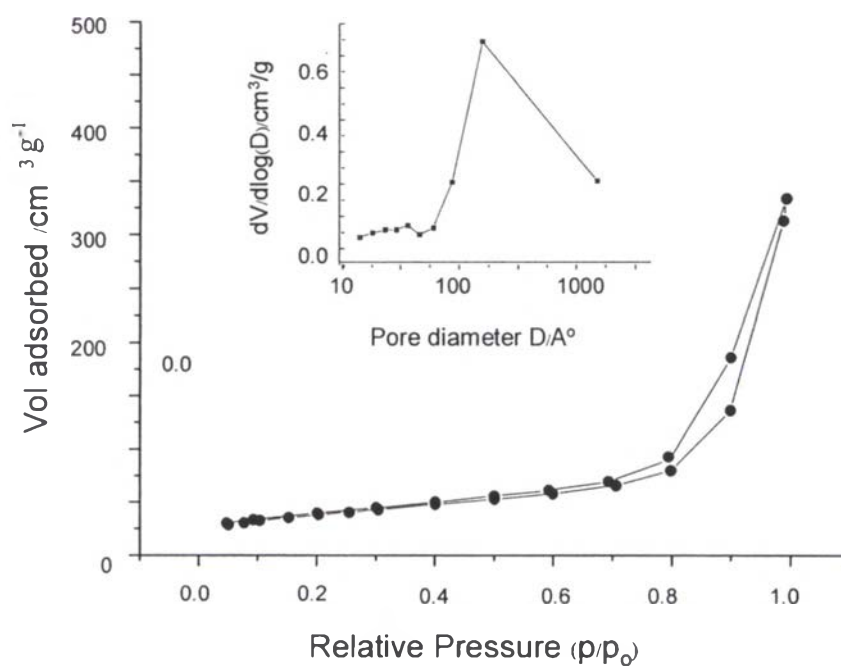and f) 200 °/1.

Figure 4.11 Nitrogen adsorption isotherm of $AlPO_4$-5 synthesized from reaction mixture composition of $Al_2O_3:P_2O_5:3.5TEA:750H_2O$ at reaction temperatures of 200 °C for 1 h. Insert is the corresponding pore size distribution.

Table 4.1   %crystallinity of the AFI products synthesized from the mixture of $Al_2O_3:P_2O_5:3.5TEA:750H_2O$ for 1 h at different microwave temperatures.

Reaction Temperature	Crystallinity (%)[*]
180°C	31.05
190°C	73.03
200°C	84.37

[*] The 100% crystallinity of AFI crystals was obtained from the sample synthesized at the mixture composition of $Al_2O_3:P_2O_5:3.5TEA:750H_2O$ at 200 °C for 1 h with the addition of HF acid.